

Computational capacity of life in relation to the universe

Philip Kurian*

As physical systems, all life in the universe processes information according to physical laws. Estimates for the computational capacity of living systems generally assume that the fundamental information-processing unit is the Hodgkin-Huxley neuron, thereby excluding aneural organisms. Assuming the laws of quantum mechanics, the relativistic speed limit set by light, a universe at critical mass-energy density, and a recent experimental demonstration of single-photon superradiance in cytoskeletal protein fibers at thermal equilibrium, it is conjectured that the number of elementary logical operations that can have been performed by all eukaryotic life in the history of Earth, which is shown to be approximately equal to the ratio of the age of the universe to the Planck time, is about the square root of the number by the entire observable universe from the beginning. The existence of ultraviolet-excited $|W\rangle$ states in these protein fibers, operating within two orders of magnitude of the Margolus-Levitin speed limit, motivates state-of-the-art performance comparisons with contemporary quantum computers.

Copyright © 2025 The Authors, some rights reserved; exclusive licensee American Association for the Advancement of Science. No claim to original U.S. Government Works. Distributed under a Creative Commons Attribution NonCommercial License 4.0 (CC BY-NC).

INTRODUCTION

All physical systems process information and can therefore be considered as performing computations. The universe and all organisms within it are physical systems, having physical attributes. Thus, they can be considered as performing computations. Physical systems performing computations obey physical laws. Here, we assume (a) the laws of quantum mechanics, (b) the relativistic speed limit set by light, (c) a matter-dominated universe at critical mass-energy density, and (d) a recent experimental confirmation from the author's group and coworkers (1), demonstrating the existence of stable superradiant states in protein systems at thermal equilibrium. By applying the Margolus-Levitin theorem (2) derived from (a), revisiting previous arguments (3) using (b) and (c), and bringing insights from experiment via (d), this article conjectures that the number of elementary logical operations that can have been performed by the universe $(t_\Omega/t_p)^2 \approx 10^{120}$ is approximately the square of the number of operations that can have been performed by all kingdoms of life on Earth in the entire existence of our planet $t_\Omega/t_p \approx 10^{60}$, a drastically revised update for the computational capacity of life $(t_\Omega/t_p)^{2/3} \approx 10^{40}$ calculated assuming a maximum information-processing speed set by all Hodgkin-Huxley neurons in animals firing at millisecond timescale. Here, $t_\Omega = 13.8 \times 10^9$ years = 4.352×10^{17} s is the age of the universe, and $t_p = \sqrt{G\hbar/c^5} = 5.391 \times 10^{-44}$ s is the Planck time.

The calculations made here thus relate the amount of computation that can have been performed by all carbon-based life in the history of the Earth, to the amount of computation that can have been performed by the part of the universe with which we are causally connected (i.e., the part within our observable horizon, from the time of the big bang to t_Ω). Comparisons are also made to classical digital computers and future quantum computers, deriving distinct estimates for the times to singularity when the number of elementary logical operations performed by the machines equals t_Ω/t_p .

Life and the universe as physical computing systems

Quantum speed limits on computation

Margolus and Levitin (2) proved that physical systems have a minimum time required to evolve between two orthogonal states (e.g., $|0\rangle$ and $|1\rangle$). According to Heisenberg, pairs of noncommuting observables will have the product of their uncertainties bounded from below by a value proportional to their commutator. The product of momentum and position has the same units as the product of energy and time, which naively implies the existence of an energy-time uncertainty relation given by

$$\Delta E \Delta t \geq \hbar/2 \quad (1)$$

where Δ signifies the variance of the quantity. However, the time variable t in Eq. 1 shows up as a continuous parameter in the Schrödinger equation, not as an operator with commutation relations, and so this energy-time uncertainty has been the subject of considerable debate since early works by Aharonov and Bohm (4, 5).

By evolving a quantum state $|\psi(0)\rangle = \sum_n c_n |E_n\rangle$ into $|\psi(t)\rangle = \sum_n c_n \exp(-iE_n t/\hbar) |E_n\rangle$ and considering the inner product $\langle\psi(0)|\psi(t)\rangle = \sum_n |c_n|^2 \exp(-iE_n t/\hbar) = 0$ for the smallest value of t , one can prove the Margolus-Levitin theorem (2). See the Methods for a complete proof and for its application to macroscopic systems. This theorem provides a strict lower bound on the time required to distinguish two orthogonal states and is given by

$$\tau \geq \frac{\pi\hbar}{2\langle\mathcal{E}\rangle} \quad (2)$$

where $\langle\mathcal{E}\rangle$ is the average energy, the expectation value of a time-independent Hamiltonian where the ground-state energy is set to zero. Similar bounds have been demonstrated to hold in classical systems, systems that operate on nonbinary or continuous variables, and across the quantum-to-classical transition (6, 7). It is thus important to stress that such "quantum" speed limits are not derived from operator noncommutativity but rather from dynamical properties of systems in Hilbert space, even when applied to the classical Liouville equation or the stochastic Fokker-Planck equation (7).

Quantum Biology Laboratory, Howard University, Washington, DC 20060, USA.

*Corresponding author. Email: pkurian@howard.edu

The maximum number of operations per unit time that can be performed by such a physical system, according to Eq. 2, is then given by

$$N_{\max} = (\tau_{\min})^{-1} = \frac{2\langle \mathcal{E} \rangle}{\pi\hbar} = \frac{2\rho c^2 \times V}{\pi\hbar} \quad (3)$$

where ρ is the rest mass-energy density and V is the volume of the system. Of course, for most physical computing systems, the majority of their energy is locked up in mass for reliability and redundancy, leaving only a tiny fraction available for performing logic. For example, billions of electrons (many redundant degrees of freedom) are used in silicon-based computers to register one single bit. Available energy thus limits the information-processing rate of a physical computing system. However, the laws of physics do not require redundancy to perform logical operations (3, 8), so the present discussion is focused on the maximum allowable speed limits for various computing substrates (observable universe, living systems, and human-made machines) obeying the Margolus-Levitin bound. Similarly, while the maximum entropy of a physical system determines the amount of information it can process in principle, controllable degrees of freedom limit the number of logical bits a physical computer can register in practice.

Upper bound on the number of operations in the matter-dominated universe

For the matter-dominated universe as a whole, this discussion follows the work of Lloyd (3, 8) and neglects the effects of physical degrees of freedom outside 3 + 1 dimensions, beyond the observable horizon of our present universe, beneath the Planck scale, and involving dark matter and dark energy. A critical density $\rho_c = \frac{3}{8\pi} H^2 / G \approx 9 \times 10^{-27} \text{ kg/m}^3$ can be derived from cosmic microwave background data, assuming that a galaxy near our observable horizon at a distance R moves away with speed HR , where H is the Hubble constant, and that the galaxy's kinetic energy $mH^2R^2/2$ and gravitational energy $Gm\rho_c 4\pi R^3/3R$ are equal. In the ensuing analysis, all factors of 2, 4/3, π , etc., will be dropped for clarity of exposition, as the arguments will be made at the approximate (\approx) order-of-magnitude scale. As a result, recent debates about the so-called "Hubble tension" (9, 10)—a discrepancy between measurements of the Hubble constant from the Planck satellite ($H = 67.4 \text{ km/s/Mpc}$) and those from the Hubble Space Telescope supported by the Dark Energy Spectroscopic Instrument ($H = 76.5 \text{ km/s/Mpc}$)—will not affect the discussion below, given that this 13.5% increase cannot alter the order of magnitude of $t_\Omega = 1/H$. A brief remark on how the Hubble tension affects other quantities is provided in the "Conjecture relating life's computational capacity to the universe's" section.

Because the age of our observable universe $t_\Omega = R/v = R/HR = 1/H$, we find

$$\rho_c \approx H^2/G = (Gt_\Omega^2)^{-1} \quad (4)$$

With the volume of the observable universe given by $V_\Omega \approx (ct_\Omega)^3$, and using Eqs. 3 and 4, we obtain the maximum number of operations that can have been performed in the history of the open, matter-dominated universe

$$N_\Omega t_\Omega \approx \frac{\rho_c c^2 \times (ct_\Omega)^3}{\hbar} t_\Omega = \frac{c^5 t_\Omega^2}{G\hbar} \quad (5)$$

This formula gives us the maximum number of ops for the universe in terms of its age and the fundamental physical constants c, G, \hbar . We can rewrite Eq. 5 as

$$N_\Omega t_\Omega \approx \left(\frac{t_\Omega}{t_p} \right)^2 = \frac{A_\Omega}{\ell_p^2} \quad (6)$$

where $t_p = \sqrt{G\hbar/c^5} \approx 10^{-43} \text{ s}$ is the Planck time, $A_\Omega = (ct_\Omega)^2 \approx 10^{52} \text{ m}^2$, and $\ell_p = ct_p \approx 10^{-35} \text{ m}$ is the Planck length. The suggestive notation of Eq. 6 hints at a holographic principle (11) for the boundary of the universe, and per the Bekenstein bound (12–14) attained by black holes and other objects with event horizons. We thus arrive at a value of $\sim 10^{120}$ to 10^{123} [dependent on inclusion of $\mathcal{O}(1)$ numerical factors] for the total operations that can have been performed in the history of the entire matter-dominated universe. Per the rightmost equality in Eq. 6, this value is also the maximum number of bits registered by the universe using matter, energy, and gravitational degrees of freedom (3). This value also exceeds the number of protons in the universe by a factor of $\sim 10^{40}$, which is consistent with extra degrees of freedom added by the fields.

Our universe is close to its critical mass-energy density, but a matter-dominated universe whose density is higher than the critical density would be closed: spatially finite, expanding to a maximum length scale over a time T , and temporally finite, recontracting to a singularity over a time $2T$. The total number of operations that can be performed over the entire history of such a closed, matter-dominated universe is given by

$$\frac{Mc^2}{\hbar} \times 2T = \frac{8\pi c^5 T^2}{3G\hbar} \approx \left(\frac{T}{t_p} \right)^2 \quad (7)$$

which is comparable in form to Eq. 6 for an open, forever expanding universe. The formula in Eq. 6 can be shown to hold also in the radiation-dominated and inflationary universes (3, 15), though the degrees of freedom for computation will be contained in vastly different forms. In particular, the radiation-dominated universe is a hostile environment for the formation of the delicate structures and processes of life, while the inflationary universe primarily produces from a highly ordered initial state large quantities of spatial volume, to generate bits for future computation.

The amount of information in bits that can be registered by a physical system is

$$I = \frac{S(\mathcal{E})}{k_B \ln 2} \quad (8)$$

where $S(\mathcal{E})$ is the thermodynamic entropy of a system with expectation value of the energy, $\langle \mathcal{E} \rangle$. For a black hole of mass m at the Schwarzschild radius $R_S = 2Gm/c^2$, the amount of information that can be stored is given by the Bekenstein-Hawking entropy, $S = k_B A / 4\ell_p^2$ such that

$$I_{\text{BH}} = \frac{4\pi Gm^2}{\hbar c \ln 2} \approx \left(\frac{m}{m_p} \right)^2 \quad (9)$$

where $m_p = \sqrt{\hbar c/G} = 2.176 \times 10^{-8} \text{ kg}$ is the Planck mass, and the quadratic scaling of m/m_p mirrors that for the maximum number of ops for the open universe in terms of t_Ω/t_p given in Eq. 6, or for the closed universe in terms of T/t_p given in Eq. 7. Using Margolus-Levitin for the number of ops that can be performed per second, we see that when it is using all its memory, the maximum number of ops per bit per second that a physical computing system can perform is

$$N_{\max} / I = \frac{2\langle \mathcal{E} \rangle k_B \ln 2}{\pi \hbar S} \propto \frac{k_B T}{\hbar} \quad (10)$$

where integrating the relationship $1/T = \partial S / \partial \mathcal{E}$ over \mathcal{E} gives the proportionality in Eq. 10 for the temperature of the system in a maximum entropy state. Thus, while the entropy S in Eqs. 8 and 9 governs the amount of information the system can register, the temperature T governs the number of ops per bit per second that it can perform. Put succinctly: Entropy limits memory, and energy limits speed.

It has been shown (16) that an upper bound v on the speed of sound in condensed phases and elemental solids can be derived in terms of these fundamental constants (see the “Conjecture relating life’s computational capacity to the universe’s” section) and features in several of their thermodynamic properties. For example, the low-temperature entropy per volume is given in terms of this upper bound by $S/V = \frac{2\pi^2}{15} k_B \left(\frac{k_B T}{\hbar v} \right)^3$, which in the regime where this formula is applicable would transform Eq. 10 to

$$N_{\max}/I = \frac{15\ln 2}{\pi^3} \frac{\omega(\rho)}{V} \left(\frac{\hbar v}{k_B T} \right)^3 \quad (11)$$

where $\omega(\rho) = \frac{\rho c^2 \times V}{\hbar}$ is the frequency associated with the volumetric rest mass-energy density. Note that the upper bound v for the speed of sound in atomic hydrogen (16) yields the maximum computational capacity per bit in the low-temperature regime by minimizing the entropy per volume at a given temperature. Comparing Eq. 11 with the proportionality in Eq. 10, we see that specific structural features of nonrelativistic materials can give vastly different scalings for their computational capacities under distinct environmental conditions.

The minimum time t_{\log} it takes for a single logical operation to flip a bit is the inverse of the quantity in Eq. 10. The degree of parallelization in a physical computing system (8) can be measured by the ratio between the minimum time it takes to communicate across the system of radius R ($t_{\text{com}} = 2R/c$), and t_{\log} , yielding

$$\frac{t_{\text{com}}}{t_{\log}} = \frac{4R\langle\mathcal{E}\rangle k_B \ln 2}{\pi \hbar c S} \propto \frac{R k_B T}{\hbar c} \quad (12)$$

When considered again in the low-temperature regime, the degree of parallelization assuming a spherical computing volume becomes

$$\frac{t_{\text{com}}}{t_{\log}} = \frac{45R\langle\mathcal{E}\rangle \ln 2}{2\pi^4 \hbar c} \left(\frac{\hbar v}{R k_B T} \right)^3 \quad (13)$$

highlighting the distinct limits in condensed phases and elemental solids. However, in general, the ordinary Coulomb electrostatic interaction between two charged particles (e^2/r) determines the minimum amount of time per bit $t_{\log}/I = \pi \hbar r / 2e^2$ it takes to perform a quantum logic operation, such as CNOT, on the two particles. Thus, the degree of parallelization from Eq. 12, $\frac{t_{\text{com}}}{t_{\log}/I} = \frac{r/c}{\pi \hbar r / 2e^2} =$

$2e^2 / \pi \hbar c = 2\alpha / \pi$, where $\alpha = e^2 / \hbar c \approx 1/137$ is the fine-structure constant, showcases the intertwined nature of the laws of electromagnetism and the limits of computation. The amount of information registered by any two particles on average must be $I < 2\alpha/\pi \ll 1$ bit for the system to execute parallel operations. Although maximum allowable memory space is given by the entropy of a system’s thermal equilibrium state, it is discussed in the next section how the actual state of a complex living system, even with many uncontrolled, atomistic thermal motions, may exhibit more controlled degrees of freedom for logical operations than previously thought,

by harnessing the interactions of quantum matter with the electromagnetic field.

Upper bound on the number of operations for carbon-based life on Earth

A collection of n two-level systems has 2^n accessible states (without superposition) and can register n bits of information, and in general a system with M accessible states can register $\log_2 M$ bits of information. According to recent findings by the author’s group (1, 17), many protein polymers comprise enormous networks of such two-level quantum emitters (a small molecule called tryptophan), and can be treated effectively as open quantum systems interacting with their environments. They are therefore subject to similar quantum speed limits on their computational capacity and exhibit observable quantum enhancements, even at thermal equilibrium or at high temperatures where the quantum-to-classical transition takes place. These protein polymers, which are ubiquitous across all eukaryotic and even some bacterial species, exhibit superradiance (18) in the single-photon limit, where sharing a single photon coherently across n quantum emitters increases the spontaneous emission rate from γ for the single emitter up to a maximum of $n\gamma$ for the collective. Single-photon superradiance (19) is thus a distinctively quantum effect, which will be shown to drastically increase estimates for the computational capacity of neural and aneural organisms.

The most recent census of Earth’s biomass concludes that there is ~ 550 gigatons of carbon ($\text{Gt C} = 10^{15} \text{ g C}$) distributed among all kingdoms of life on our planet (20). Plants form the bulk of this carbon-based life at ~ 450 Gt C, followed by bacteria at ~ 70 Gt C. Fungi, archaea, and animals follow further behind, totaling only ~ 20 Gt C.

The proteins studied by the author’s group (1, 17) form vast cytoskeletal architectures across almost all domains of carbon-based life, and they exhibit single-photon superradiance. That is, even in the limit of a single photon shared coherently across n quantum two-level systems, these protein architectures support superradiant states (with radiative decay rates $n\gamma > \Gamma_j > \gamma$ for each state j) that are strongly coupled to the electromagnetic field due to their collective long-range interactions. The fluorescence quantum yield, in particular, is a good figure of merit for this effect because in these architectures the quantum yield exhibits considerable resilience to thermal disorder due to the selection for the brightest superradiant states in the lowest-energy portion of their spectra, which is weighted more strongly in the thermal Gibbs ensemble (1, 17) as $\propto \exp(-E_j/k_B T)$. As a consequence, the fluorescence quantum yield has been experimentally confirmed to show clear signatures of superradiant enhancement at room temperature (1). This result provides strong evidentiary support that, even in the presence of uncontrolled thermalized degrees of freedom, certain quantum degrees of freedom in the protein architectures of carbon-based life, namely, in all eukaryotic cells, can be used for logical operations and information processing, above the thermal noise floor.

Large bundles of these cytoskeletal fibers organize in neuronal axons (1), which are stable on the order of mammalian lifetimes. The upper bound for this type of superradiant computation in these protein fiber bundles, based on calculations of the state lifetimes and ultrafast transient absorption measurements on ensembles of single fibers, is $\sim 10^{13}$ operations per second (1, 17), more than a billion times faster than the computational capacity expected of a single Hodgkin-Huxley neuron ($\sim 10^3$ operations per second) spiking according to conventional ionic action potentials. As these superradiant states are stimulated by ultraviolet photons (~ 4.4 eV), the

Margolus-Levitin bound gives $N_{\max} \approx \langle \mathcal{E} \rangle / \hbar \approx 10^{15}$ operations per second, indicating that these protein fiber bundles are operating within two orders of magnitude of this limit (see Fig. 1). Intriguingly, in 1981, before Margolus and Levitin's proof [see Methods and (2)], Bekenstein (12) established an upper bound of 10^{15} ops/s on the speed of an ideal digital computer.

Assuming 465-Gt C eukaryotic biomass on Earth, 1- ng C per eukaryotic cell, and 100 superradiant fibers per eukaryotic cell (1000 per neuronal axon), a conservative estimate is obtained for the computational capacity of "superradiant life" on Earth: $N_E \approx 10^{41}$ ops/s. This value exceeds by more than 15 orders of magnitude the estimate for all Hodgkin-Huxley neurons, $\sim 10^{25}$ ops/s, calculated for all animals on Earth (2 Gt C) using their average brain-to-body mass ratio (10^{-2}) and the average carbon mass for a single neuron

(1 ng C). Assuming constant biomass over the age of the Earth t_E , it is found that all kingdoms of superradiant life on Earth can have performed no more than

$$N_E t_E \approx 10^{60} \text{ ops} \quad (14)$$

in the entire existence of our planet. Before the Cryogenian Period (~720 to 635 million years ago (Ma)), the relatively low and static species richness in the eukaryotic fossil record mimicked the "Boring Billion" (~1800 to 800 Ma) characterized by stable global carbon cycles (21). Even though the eukaryotic diversity pattern increased rapidly with more dynamic changes in the Ediacaran (~635 to 539 Ma) and early Cambrian (~539 to 509 Ma) periods, the assumption of constant eukaryotic biomass over the age of the Earth ensures a reasonable upper bound. However, in comparison to the present,

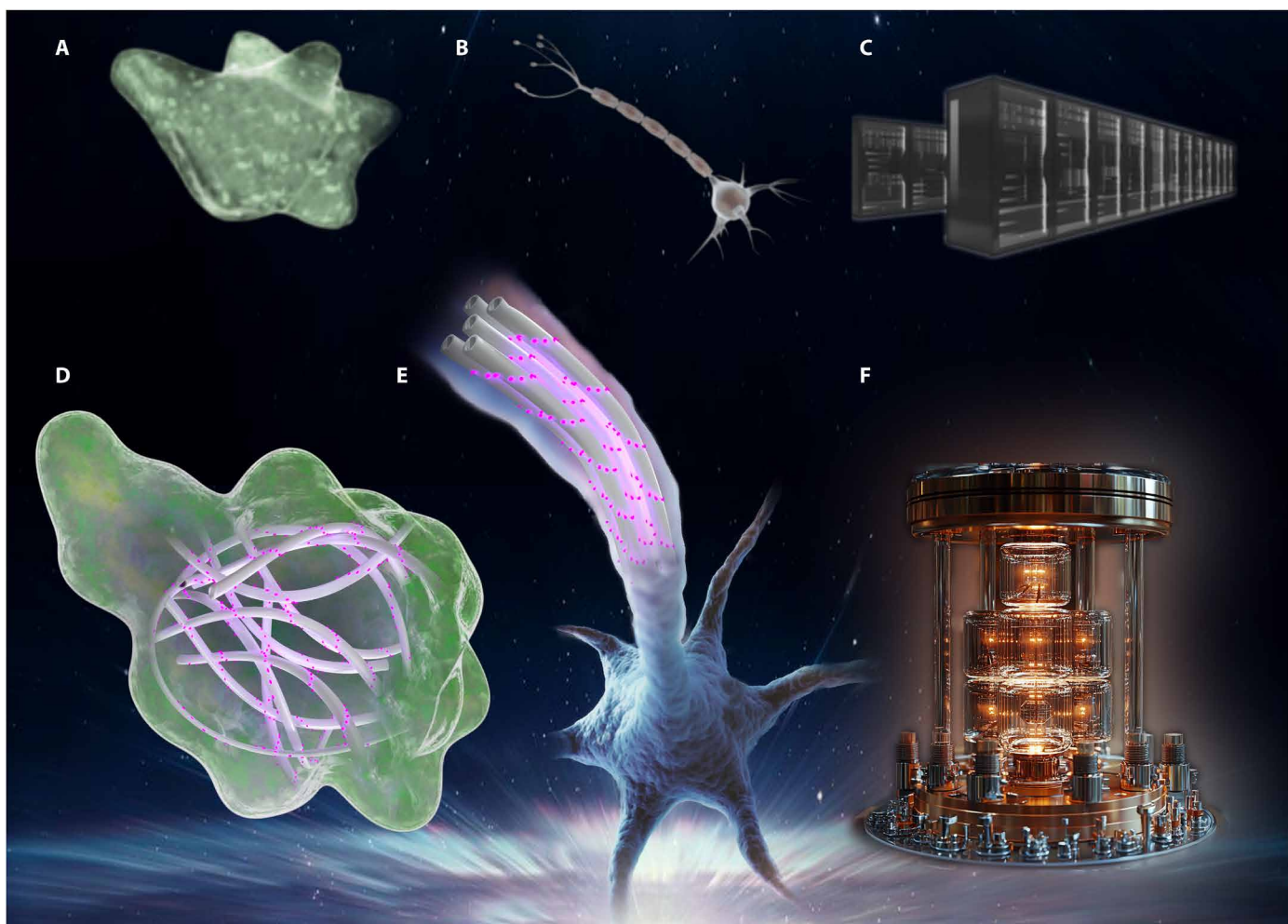


Fig. 1. Living systems maintain information-processing architectures using photoexcited quantum degrees of freedom. The computational capacities of aneural organisms (A) and neurons (B) have been drastically underestimated by considering only classical information channels such as ionic flows and action potentials, which achieve maximum computing speeds of $\sim 10^3$ ops/s. However, it has been recently confirmed by fluorescence quantum yield experiments (1) that large networks of quantum emitters in cytoskeletal polymers support superradiant states at room temperature, with maximum speeds of $\sim 10^{12}$ to 10^{13} ops/s, more than a billion times faster and within two orders of magnitude of the Margolus-Levitin limit for ultraviolet-photoexcited states. These protein networks of quantum emitters are found in both aneural eukaryotic organisms (D) as well as in stable, organized bundles in neuronal axons (E). In this work, quantitative comparisons are made between the computations that can have been performed by all superradiant life in the history of our planet, and the computations that can have been performed by the entire matter-dominated universe with which such life is causally connected. Estimates made for human-made classical computers (C) and future quantum computers with effective error correction (F) motivate a reevaluation of the role of life, computing with quantum degrees of freedom, and artificial intelligences in the cosmos.

potentially lower numbers of eukaryotes before the Cryogenian, and multiple extinction events after, would tighten the upper bound in Eq. 14, but likely by less than an order of magnitude.

Where might these superradiant networks have arisen from? The vast cytoskeletal architectures of quantum two-level emitters found in eukaryotic life may have emerged from rather distinct architectures observed at astronomical scales. So-called astronomical polycyclic aromatic hydrocarbons (astroPAHs), essentially flakes and clusters of fused benzene and other aromatic rings, appear to be fragmented into smaller astroPAHs in the interstellar medium under exposure to ultraviolet photons (22). The strong radiation field can remove peripheral hydrogen atoms and then amputate dangling carbons, creating pentagons in the otherwise hexagonal graphene lattices. Further astroPAH degradation and astrochemistry can result in the formation of the quantum emitter tryptophan, a bicyclic aromatic consisting of a hexagonal benzene ring fused to a pentagonal pyrrole ring. There has been lively debate over the recent claim that tryptophan has been spectrally identified in the interstellar medium (23–25), as such a discovery would provide strong support for the exogenous origin of meteoritic amino acids and the seeding of pre-biotic conditions for life on Earth.

RESULTS

Conjecture relating life's computational capacity to the universe's

Given Eq. 14, consider the following approximate relation

$$10^{120} \approx N_\Omega t_\Omega \stackrel{?}{=} (N_E t_E)^2 \approx (10^{60})^2 \quad (15)$$

Using Eqs. 6 and 15 above, the author proposes the following conjecture relating the computational capacity of life to the computational capacity of our observable universe respecting quantum mechanics

$$\left(\sqrt{\Lambda} \ell_p\right)^{-1} \approx \left(\frac{e^2}{G m_e m_p}\right)^{\frac{3}{2}} \approx \sqrt{N_\Omega t_\Omega} \approx N_E t_E \approx \frac{t_\Omega}{t_p} \quad (16)$$

where $\Lambda \approx 10^{-52} \text{ m}^{-2}$ is the cosmological constant, and $e^2 / G m_e m_p \approx 10^{40}$ is the ratio between the electromagnetic and gravitational forces between an electron and a proton (with $4\pi\epsilon_0 = 1$), also known as the Eddington-Dirac large number (26–29). The conjecture in Eq. 16 relates the largest (cosmological) and smallest (Planck) scales in the physical universe, through superradiant life. This conjecture is robust over the lifetime of the Earth (at least for the next 1 billion years) but will be altered ultimately by the details of the carbonate-silicate geothermal cycle.

Given that the upper bound for the speed of sound in condensed phases and elemental solids has been found in terms of such fundamental constants, with

$$\nu = \alpha c \left(\frac{m_e}{2m_p}\right)^{\frac{1}{2}} \approx 36,101 \frac{\text{m}}{\text{s}} \quad (17)$$

in atomic hydrogen (16), this conjecture can also be rewritten as follows

$$\left(\sqrt{\frac{\alpha^3}{2}}\right)^3 \left(\frac{m_p}{m_p}\right)^3 \left(\frac{c}{\nu}\right)^3 \approx N_E t_E \approx \frac{t_\Omega}{t_p} \quad (18)$$

The fine structure constant α , the ratio of the Planck mass to the proton mass $[m_p/m_p \approx 10^{20} \approx (t_\Omega/t_p)^{1/3}]$, and the ratio of the speed of light in vacuum to the maximum speed of sound in atomic hydrogen ($c/\nu \approx 8304$) are prominent factors in this reformulation. They highlight, respectively, the role that the electromagnetic field, quantum mechanics, and relativity play in both the evolution of living matter and of all matter in the universe. Of course, mechanical processes governing the speed of sound in molecular solids, crystals, and liquids are much slower than the speed of light, so it may initially be unexpected to see ν occur in the estimate 18 for the computational capacity of life. The most critical factor, however, is m_p/m_p scaled cubically rather than quadratically (see Eqs. 6, 7, and 9), and contains, implicitly, the constants \hbar , c , and G , integrating quantum mechanics, relativity, and gravity with the mass m_p of the fundamental positively charged baryon in elemental nuclei.

Rewriting the rightmost equality of the conjecture in Eqs. 16 and 18 as

$$N_E \approx \frac{t_\Omega}{t_E t_p} \quad (19)$$

we can compare the upper bound computing speed of life with the upper bound computing speed of the universe, $N_\Omega \approx t_\Omega(t_p)^{-2}$. $N_\Omega \approx 10^{104}$ ops/s is of course cosmically larger, by more than 60 orders of magnitude, than $N_E \approx (t_p)^{-1}$. Note that in Eq. 19, $t_\Omega/t_E \approx 3$, but this ratio will decrease to a minimum value of ~ 1.64 over the next 10 billion years, the upper-bound timescale for extinction of all life on Earth. Given the 13.5% discrepancy highlighted in the “Upper bound on the number of operations in the matter-dominated universe” section by the Hubble parameter tension, the age of the universe $t_\Omega = 1/H$ to the best of our knowledge is uncertain within about 1.73 billion years. Thus, the ages of the universe and of Earth being within one order of magnitude, the minimum value attained by t_Ω/t_E in the next 10 billion years could vary between ~ 1.57 and ~ 1.69 .

A rather general analysis of quantum clocks given by Wigner (30) found that the running time $T < m\ell^2/\hbar$, for a clock of mass m and linear extent ℓ . As T divided by the number of orthogonal states over which the clock system can run gives its time accuracy t , we can estimate that a cytoskeletal fiber of $\ell = 1 \mu\text{m}$ and a total mass of 10^{-7} ng , with 10^4 distinct (pointer) states, would exhibit a time accuracy of $t = T/n \approx m\ell^2/\hbar = 95 \text{ ms}$, about the average duration of a human eye blink and overlapping with the subradiant state lifetimes calculated for representative structures (17). For a sensory neuron ($m = 10 \text{ ng}$) in small invertebrates ($\ell = 1 \text{ cm}$), the time accuracy t approaches just a little over 1 day when the number of distinct pointer states grows to 10^{14} , suggesting a curious relationship to the circadian cycle and a 10-orders-of-magnitude augmentation of the states with even a small fraction of the Hilbert space (2ⁿ). In the weak-excitation regime where $0 < n \lesssim 10^2$ represents the effective number of two-level systems (qubits) over which orthogonal excited states form, such a neuronal quantum clock's accuracy can be brought to the picosecond scale. Converting the Wigner inequality into an equally crude frequency bound (31) gives $1/T > \hbar/m\ell^2$, which corresponds to a period of approximately 16 min for the cytoskeletal fiber considered above, just an order of magnitude difference compared to the longest subradiant state lifetimes calculated in bundled fibers from detailed numerical simulations (1). These estimates suggest a robust hierarchy of timescales

across which quantum biological clocks can operate over an organismal lifetime.

Comparisons with classical and quantum computing machines

In 1961, Landauer (32) showed that reversible (one-to-one) logical operations such as NOT, CNOT, and CCNOT (Toffoli) can be performed, in principle, without dissipation, but that irreversible, many-to-few operations such as AND, NAND, OR, and XOR require dissipation of at least $k_B \ln 2$ for each bit of information lost. Essentially, the one-to-one dynamics of Hamiltonian systems implies that when a bit is erased, the information that it contains has to go somewhere. If the information goes into observable degrees of freedom of the computer, such as another bit, then it has not been erased but merely moved. However, if it goes into unobservable degrees of freedom such as the microscopic motion of molecules or unspecified modes of the electromagnetic field, it results in an increase of entropy of at least $k_B \ln 2$. For a deterministic many-to-few mapping of initial states with nonzero probabilities into a smaller number of final states, the entropy decreases and $S_f < S_p$, so the entropy of the surrounding thermal environment must increase by at least $|S_i - S_f|$ for the second law of thermodynamics to hold for the closed system + environment. While Landauer's principle is generally expressed as an environmental heating requirement of $k_B T \ln 2$ per bit lost in the operation, a clearer statement of the principle is given by

$$Q_{\text{env}} \geq k_B T |I_i - I_f| \ln 2 \quad (20)$$

per Eq. 8 for the information lost in the process, which reduces to the conventional lower bound when considering the dissipative cost of logically irreversible operations where $I_i = 1$ bit and $I_f = 0$ for a well-defined final state.

For a typical irreversible computer, at least one bit per elementary logical operation is usually discarded, as is the case when two input states map to a single output state. In the irreversible operation cases listed above, the number of distinct input states over n classical bits is 2^n , but the number of distinct output states is always 2 (0 or 1), thus sacrificing an exponentially larger amount of information. However, far less than one bit per operation can be lost on average when the input probability distribution is highly skewed or nonuniform, and the information loss is $I_i - I_f \ll 1$ bit. Recall that the amount of information registered by two charged particles was shown above to require on average far less than one bit to execute parallel operations. Nonuniform input distributions can thus yield dissipation bounds lower than $k_B T \ln 2$ per operation with no violation of Landauer's principle.

Such nonuniformities can arise in simulacra of complex living systems coevolving in tight connection with their environments. Variants of cellular automata (CA) from Conway's "The Game of Life" (33) have demonstrated both unbounded evolution (a lack of repeating patterns within the expected Poincaré recurrence time of an isolated system) and innovative or novel trajectories in open CA systems coupled to an elementary "environmental" CA (34). These CA can remarkably capture some features of evolutionarily conserved enzymes and their biomolecular networks.

In his 1973 paper on reversible computation (35), Bennett mistakenly equated the action of the enzyme RNA polymerase with an idealized tape-copying Turing machine, which is strictly reversible, both logically and thermodynamically. RNA polymerase, which transcribes messenger RNA from DNA, is not thermodynamically reversible, even though the DNA sequence from which the mRNA is constructed does exhibit a one-to-one correspondence. As with most biological

reactions, energy is dissipated by RNA polymerase and many other enzymes at a rate of roughly $10 k_B T$ per step, distinguishing their operation from the thermal noise floor $k_B T$ (~ 0.02 eV) at the price of each of the phosphodiester bonds (~ 0.2 eV), which join the nucleotides of RNA and DNA, and nearly the cost of a phosphoanhydride bond (~ 0.3 eV) in the biomolecular energy currency adenosine triphosphate.

If CA used to describe this biomolecular machinery are governed by quantum mechanical rules such that given sites are permitted to exist in a superposition of probability amplitudes, wave-like structures and interference patterns characteristic of quantum coherence have been shown to emerge (36).

Computing with coherence

If we specify a quantum state (or ensemble of states) with a density matrix ρ defined by the basis states $|i\rangle$, the coherence length is given by

$$L_\rho = \frac{1}{n} \frac{\left(\sum_{i,j} |\rho_{ij}| \right)^2}{\sum_{i,j} |\rho_{ij}|^2} \quad (21)$$

which in the single-excitation manifold measures how much a single excitation is spread coherently over the sites composing the aggregate. A pure localized state, for which $\rho = |i\rangle \langle i|$, thus attains a minimum value $L_\rho = 1/n$, while a fully delocalized coherent state characterized by $\rho = 1/n \sum_{i,j} |i\rangle \langle j|$ achieves the maximum value $L_\rho = n$. The latter holds for so-called $|W\rangle$ states, which include superradiant and subradiant states in the single-excitation limit, but also for any pure state with constant amplitude $1/\sqrt{n}$ over the sites and with arbitrary phases. In between these two extreme values, a completely delocalized mixed state characterized by $\rho = 1/n \sum_i |i\rangle \langle i|$ has $L_\rho = 1$ from Eq. 21, being maximally delocalized in the site basis but completely incoherent (lacking off-diagonal elements).

The von Neumann entropy, $S(\rho) = -k_B \text{tr}(\rho \ln \rho)$, for each of the three types of density matrices described below Eq. 21 gives 0 for the pure localized state, $k_B \ln n$ for the maximally delocalized, completely incoherent mixed state, and 0 for the maximally coherent $|W\rangle$ state. Only in quantum mechanics can the entropy of such a combined (coherent) system be less than the sum of the entropies of its components. For a many-to-one mapping between a mutually orthogonal set of initial pure localized states and a final $|W\rangle$ state (or any other pure state), $I_i - I_f = 0$, so there is no lower bound on Q_{env} , as given by Eq. 20. If the number of qubits remains constant during the process, then this many-to-one mapping is logically reversible, with no entropy increase. In other words, given a set of input single-excitation basis states $|100 \dots\rangle, |010 \dots\rangle, \dots, |0 \dots 01\rangle$, a unique output $|W\rangle$ state is readily constructed. Quantum systems exploiting these properties can thus operate extremely efficiently, near or beyond the Landauer bound.

However, this many-to-one process is not physically reversible, as measurement "collapse" or state update via the Born rule from the $|W\rangle$ state to any one pure localized state is highly nonlinear, contrary to the unitary evolution prescribed by the Schrödinger equation. Strictly speaking, quantum measurement (state reduction) of the $|W\rangle$ state to a pure localized state does not alter the von Neumann entropy ($= 0$), but deterministic control is not possible in the ensemble of identically prepared $|W\rangle$ states and will generally produce an incoherent mixed state after state reduction, increasing the von Neumann entropy to its maximum value of $k_B \ln n$. As qubits are

removed from the system in a maximally delocalized, completely incoherent mixed state, its von Neumann entropy decreases with $k_B \ln n$, such that $\dot{S}(\rho) = k_B \dot{n} / n$. As qubits are removed from a $|W\rangle$ state, its von Neumann entropy remains zero (still a pure state), and it retains its maximal entanglement across the remaining qubits as ancillary qubits are sacrificed, erased, or lost from the system at the rate \dot{n} . In other words, if you have a $|W\rangle$ state and measure ancilla qubits all to $|0\rangle$, the remaining qubits are still in a $|W\rangle$ state, but of reduced dimension. It has been shown (37) that the entanglement of the $|W\rangle$ state is maximally robust under qubit disposal, and that it is inequivalent to the Greenberger-Horne-Zeilinger state under local operations with classical communication.

Coherences of $|W\rangle$ and $|W\rangle$ -like states in the low-lying energy levels of their spectra can be exploited in a nonequilibrium context, where an energy source of hot thermal photons coexists with an entropy sink of cold photons. In this scenario, “noise-induced” radiative quantum coherence can break detailed balance to extract more power from the system (38). This effect can be robust against environmental decoherence. It has been suggested (31) that living organisms can exploit such thermodynamic gradients to drastically reduce the effective temperature of biomolecular complexes to the millikelvin scale, including in the cytoskeletal fibers described by the author’s group (17).

If a physical computing system is subject to an error rate of ϵ bits per second, then error-correcting codes can be used to detect those errors and reject them to the environment at a dissipative cost of $\epsilon k_B T \ln 2$ joules per second, where T is the temperature of the environment. A calculation of the rate that a physical computing system must reject errors to the environment to maintain reliable behavior (8) indicates the necessity of operating at a slower speed than the maximum allowed by the laws of physics. Even if an extremely low error rate is achieved, the energy throughput required (intake of free energy and expulsion of thermal energy) demands that the system turn over its entire rest mass energy in very short periods of time.

Living systems as physical computers must reject errors to the environment at a high rate to maintain reliable function. At $T = 310$ K, $\epsilon k_B T \ln 2$ should be greater than 3×10^{-21} watts (~ 0.02 eV per second), to reject errors to the environment at a rate of $\epsilon > 1$ bit per second. For the ultraviolet-photoexcited states the author’s group considered in single-axon protein fiber bundles (1), subpicosecond superradiant pulses with power outputs in the microwatt regime correspond to error-correction rates of up to $\sim 10^{14}$ bits per second. Each single-axon protein fiber bundle performing a maximum of $\sim 10^{13}$ operations per second, even with up to 10 bits of error per operation, is thus able to avoid overheating. Over the whole human brain ($\sim 10^{11}$ neurons), the error-correction rate is $\lesssim 10^{25}$ bits per second, rejecting errors to the environment at an energy exchange of up to a maximum of $\sim 10^5$ watts! This is an order of magnitude more than the average photosynthetic power output per square kilometer of land, and two orders of magnitude greater than the synchrotron radiation power loss per ring in the Large Hadron Collider at 7000 GeV. A maximally superradiant human brain, operating in such a pulsed fashion, would turn over just 0.1 % of its total rest mass energy ($mc^2 \approx 10^{17}$ joules) in 10^9 s, a little over 30 years. Even a factor-of-three decrease in the maximum error-correction rate would increase this value beyond most human lifetimes, a physically sustainable energy throughput indeed.

State-of-the-art realizations

Nanophotonic devices using quantum dots, with interactions mediated by ultraviolet photons, have demonstrated about 10^4 times

more energy efficiency, across a wide range of bit error rates, than the minimum dissipation required for a single bit flip by a classical logic gate (39). A reliable and scalable technique for generating on-demand $|W\rangle$ states in such nanophotonic circuits has also been demonstrated (40). The protein fibers described here are well-equipped for such a nanophotonic construction in the biological milieu of ultraweak metabolic photon emissions (41, 42), and they operate at similar energy efficiencies. Error-correcting codes in these physical computing systems function as working analogs of Maxwell’s demon, getting information and using it to reduce entropy at an energy exchange rate of at least $k_B T \ln 2$ joules per bit. From the work of Bennett (35), we know that all computations can be embedded in a logically reversible framework with sufficient algorithmic overheads, and therefore do not require dissipation in principle (see Eq. 20 when $I_i = I_f$). However, in practice, any computationally restricted agent (capable of implementing only a finite number of gates) will dissipate energy, because the unobservable degrees of freedom cannot be tracked to reversible precision at the Avogadro or thermodynamic limit ($n \rightarrow \infty$) for Hamiltonian systems. Certainly, this requirement for reversible precision at the thermodynamic limit is impossible for quantum systems obeying Heisenberg uncertainty relations.

Over the course of the last two decades, high-temperature nuclear magnetic resonance (NMR) quantum computers have fallen out of favor with respect to newer implementations that operate at very low temperatures (e.g., ion traps and superconducting circuits). Protocols designed to dynamically cool target qubits at the expense of heating up auxiliary qubits using global unitaries have been extended also to open systems (43), thereby achieving so-called “heat bath algorithmic cooling” beyond Shannon’s bound. Could superradiant life be exploiting such reservoir engineering of $|W\rangle$ states in large architectures of biological qubits (1, 17) for enhanced information processing? It has been shown (43) that, in the thermodynamic limit, the minimal value of work that must be invested to maximally cool a target qubit is $\frac{\hbar\omega}{2} \tanh(\hbar\omega/2k_B T) / (\exp(\hbar\omega/k_B T) + 1)$. Applying this formula to the ultraviolet-excited $|W\rangle$ states of biology at 310 K, the minimal work is completely negligible ($\lesssim 10^{-55}$ eV) at values of $k_B T / \hbar\omega \approx 0.006$ to 0.008, far outpacing state-of-the-art values for superconducting ($\sim 10^{-9}$ eV at $T = 6.5$ mK and $\omega = 5$ GHz, or $k_B T / \hbar\omega \approx 0.17$), neutral-atom ($\sim 10^{-9}$ eV at $k_B T / \hbar\omega \approx 0.17$), and trapped-ion ($\sim 10^{-10}$ eV at $k_B T / \hbar\omega \approx 0.12$) qubits in contemporary quantum computers (43).

This “low-temperature” behavior of biology is due to the relatively high energy of ultraviolet photoexcitations compared to thermal noise. While the crossover from slow, high-temperature scaling to fast, low-temperature scaling for dynamic cooling made the process ineffectual for early NMR quantum computers, such fast scaling enables its widespread applicability in the superradiant biosystems described here. As with the case of high-temperature superconductivity, complex states of matter and light can, in biology, also defy overly simplistic $k_B T$ reasoning.

Such simplistic reasoning has frequently raised the specter of decoherence for quantum states in biosystems. However, certain enzymatic complexes studied by the author’s group (44, 45) have demonstrated the ability to form decoherence-free subspaces in Hilbert space. Thus, they maintain quantum correlations (superposition and entanglement) in a bound substrate such as DNA, even when coupled strongly to degrees of freedom in the external environment, by steric exclusion, shielding, or modification of interfacial water layers. Strongly

interacting a system of coupled quantum harmonic oscillators with an external heat bath can effectively force disparate oscillations into synchrony to maintain a limited form of quantum coherence, not in spite but because of the environment. When strongly interacting in a sufficiently nonlinear fashion, this behavior can be described as a manifestation of the Zeno (46), Kuramoto (47), or Fröhlich (48–50) effects, effectively “steering” or “concentrating” the quantum correlations of the system toward a specified, coordinated function across many degrees of freedom in the complex free-energy landscape.

A natural (and simultaneously teleological) question now arises: If life and the universe are performing sophisticated computations, what exactly are the functions and purposes of their computing? Neglecting dark matter and dark energy, most elementary operations in the matter-dominated universe, including life, consist of computing the dynamical evolution of protons, neutrons, electrons, and their constituent force-field carriers (gluons, photons, etc.) that govern their interactions according to physical laws, as well as computing emergent behaviors that arise in large collectives of these fundamental objects (51, 52). Note that this reply answers only the natural how part of the preceding question, but not the teleological why. In the words of one luminary of American letters (53), “But since why is difficult to handle, one must take refuge in how.” As expected, the computations required for this dynamical physical evolution dwarf the number of *in silico* digital computations or quantum computations that we normally associate with conventional human-made computers. Nevertheless, it is instructive to compare the computational capacity of these conventional computers with that of all eukaryotic life in the history of Earth.

Upper bound on the number of operations for silicon-based classical computers

Assuming Moore’s law, where about half of all elementary silicon-based logical operations have occurred in the last 2 years, and overestimating 10^{10} computers operating at exascale (10^{18} operations per second) for 10^8 s, all human-made computers can have performed no more than $N_M t_M \approx 10^{36}$ operations in the last 2 years, and no more than twice this amount in the entire history of silicon-based computation. This value includes silicon-based computers that support artificial intelligences. Clearly, human-made computers perform far fewer operations than living systems.

If we wish to know the time to singularity, where $N_M t_M$ will equal all the operations of superradiant life in the entire history of the Earth, we merely solve the following equation

$$N_M t_M \times 2^{S^*} = N_E t_E = \frac{t_Q}{t_p} \quad (22)$$

where in the rightmost equality we have used the conjecture in Eq. 16. Solving for the time to singularity t_{S^*} below, we obtain the following for the number of Moore doubling periods S^* in Eq. 22

$$t_{S^*} = 2 \text{ years} \times S^* = 2 \log_2 \frac{N_E t_E}{N_M t_M} \approx 160 \text{ years} \quad (23)$$

which is about four times larger than the time to singularity calculated assuming that life’s computational capacity is upper bounded by all Hodgkin-Huxley neurons in animal species. Including $\mathcal{O}(1)$ numerical factors and the maximum uncertainty in the age of the universe discussed in the “Conjecture relating life’s computational capacity to the universe’s” section, the estimate given in Eq. 23 only changes by about 3% to $t_{S^*} \approx 165$ years.

The rise of the (quantum) machines

Consider the classical memory required to store a fully general quantum state $|\psi_n\rangle$ of n qubits, each a two-level system. The Hilbert space for these n qubits is spanned by 2^n orthogonal states, such that $|\psi_n\rangle = \sum_{j=1}^{2^n} c_j |j\rangle$, with complex-valued amplitudes c_j . Each complex number requires two floating point numbers for $\Re(c_j)$ and $\Im(c_j)$. Using 32 bits (four bytes) for each floating point number, a quantum state of $n = 27$ qubits will require 4 bytes/float $\times 2$ floats/amplitude $\times 2^{27}$ amplitudes/quantum state ≈ 1.074 gigabytes per quantum state. Each additional qubit doubles the memory, so a quantum state of $n = 37$ qubits will require $2^{10} \approx 10^3$ times the memory, or about one terabyte. Simulating more than 50 qubits in a fully general superposition state thus represents a severe strain on current classical computational capabilities (54), requiring greater than a petabyte-scale memory. It is thus not unexpected that there is considerable debate about whether current quantum computing architectures can attain quantum supremacy over classical simulators, as benchmarking in the absence of effective quantum error correction would be impossible without classical algorithms to check the results (55).

At the time of this writing, one of the most promising implementations for effective quantum error correction uses a lattice-based surface code (56) of distance d , combining $2d^2 - 1$ multiple physical qubits into a logical qubit and exponentially suppressing the logical error rate ϵ with the addition of more qubits. The reduction in the logical error rate when increasing the code distance d by 2 is given by

$$\Lambda = \frac{\epsilon_d}{\epsilon_{d+2}} \approx \frac{(p/p_{\text{thr}})^{\frac{d+1}{2}}}{(p/p_{\text{thr}})^{\frac{d+3}{2}}} = \frac{p_{\text{thr}}}{p} \quad (24)$$

where p and p_{thr} are the physical and threshold error rates, respectively. Fault-tolerant quantum computing requires error suppression beyond breakeven of $\Lambda > 2$, and a classical coprocessor to decode syndrome errors in real time, which must keep pace with the fast error-correcting cycle times. Although this superconducting processor implementation only goes up to distance $d = 7$ with an error-correcting cycle time of 1.1 μ s, one can extrapolate that a 10^{-6} error rate would require a $d = 27$ logical qubit using 1457 physical qubits. For comparison, biological qubit architectures in eukaryotic protein fibers (1, 17) can frequently grow larger than a $d = \sqrt{\frac{n+1}{2}} = \mathcal{O}(\sqrt{n})$

logical qubit, comprising $n \gg 10^5$ physical qubits. Their error-correcting cycle times are about 1 ps (six orders of magnitude faster), per the analysis of superradiant state lifetimes given in the “Upper bound on the number of operations for carbon-based life on Earth” section and the general estimates for quantum biological clocks offered in the “Conjecture relating life’s computational capacity to the universe’s” section. As these architectures maintain interqubit spacings a in the extreme subwavelength regime ($a/\lambda \approx 1/280$), they comfortably exhibit threshold error rates $p_{\text{thr}}/p \approx \epsilon_d/\epsilon_{d+2} \gg 2$ that scale beyond breakeven, even in the limit where the system size on the order of micrometers exceeds the excitation wavelength and the maximum superradiant decay rate has not yet saturated (1, 17, 42).

Assuming Neven’s law for quantum computers, where the rate of growth is doubly exponential due to scaling with the number of qubits and with the improvements in quantum processors, and overestimating 10^4 quantum computers operating at terascale (10^{12} operations per

second) for 10^8 s, all human-made quantum computers will have performed no more than $N_Q t_Q \approx 10^{24}$ operations in the 2 years after relevant quantum supremacy with effective error-correcting codes is achieved, and no more than twice this amount in subsequent 2-year increments. The equation to solve for the time to singularity then changes as follows

$$N_Q t_Q \times 2^{S^*} = N_E t_E = \frac{t_\Omega}{t_p} \quad (25)$$

where again, in the rightmost equality, we have used the conjecture in Eq. 16. The time to singularity t_{S^*} then changes accordingly, solving for S^* in Eq. 25

$$t_{S^*} = 2 \text{ years} \times S^* = 2 \log_2 \log_2 \frac{N_E t_E}{N_Q t_Q} \approx 14 \text{ years} \quad (26)$$

which is only about 2 years more than the time to singularity calculated assuming that life's computational capacity is upper bounded by all Hodgkin-Huxley neurons in animal species. The estimate in Eq. 26 is extremely robust to changes in the t_E assumption due to the comparatively shorter time that eukaryotes have existed than the age of the planet, and it is likewise robust to inclusion of the classical machines from the "Upper bound on the number of operations for silicon-based classical computers" section, scaling according to Moore's law, which would be dwarfed in comparison to this doubly exponential rate of growth. The order-of-magnitude decrease from Eqs. 23 to 26 places the time to singularity, assuming relevant quantum supremacy is achieved in less than 20 years, within the next three decades, squarely within a single human lifetime. The rise of quantum computers will effectively degrade the distinction between superradiant life and "classical" neurochemical life, at least in terms of the time to singularity as defined here, and presuming the advent of quantum computers that can compute more efficiently than our high-performance classical ones.

As soon as this singularity is attained, another follows closely behind, when quantum machines attain the computational capacity of the observable matter-dominated universe

$$t_{S^{**}} = 2 \text{ years} \times S^{**} = 2 \log_2 \log_2 \frac{N_\Omega t_\Omega}{N_Q t_Q} \approx 17 \text{ years} \quad (27)$$

The prediction in Eq. 27 is robust to within a year over at least 30 orders of magnitude error in the estimate $N_Q t_Q$. Of course, given the uncertainty of quantum computing hardware development, these are upper bounds assuming an idealized growth law and will not be attained in practice.

Even so, while admitting the possible emergence of such a quantum supercomputing oracle, there remain opportunities for living systems to check the oracle's truth claims by entanglement-sharing schemes. With multiple classical computers, multiprover interactive proof (MIP) systems can verify hard-to-solve problems that cannot be efficiently checked in polynomial time by a single computer (beyond NP). It was shown in (57) that MIP systems using multiple quantum computers sharing entangled qubits can efficiently check an even harder-to-solve class of problems, which would require doubly exponential time to check on a classical computer (NEEXP). This result extends the potential universe of possibilities for qubit-sharing humans, if a quantum supercomputing oracle ever asserts truth claims that seem impossibly difficult to verify.

DISCUSSION

From a recent experimental validation of superradiance in room-temperature protein networks of quantum emitters (1), the author derives an upper bound on the number of computations that can have been performed by all superradiant carbon-based life in the entire history of Earth, which is ~ 20 orders of magnitude larger than the same quantity for all animal species over the same period, calculated assuming that Hodgkin-Huxley neurons set the maximum information-processing speed. From a minimum of assumptions, the author's conjecture relating the computational capacity of life to that of the universe echoes much earlier work by Dirac (29) and Dyson (58), and more contemporary suggestions by Davies (31, 59). This conjecture may stimulate further studies on the physical limits of artificial intelligences and the role of life in the evolution of the cosmos [see (60) for a prior treatment].

It is important to remember that even quantum computers operating at the physical limits of computation are much slower and process much less information than these upper bound calculations have shown, because most of their energy is locked up in mass, thereby limiting both speed and memory. Unlocking rest mass energy is of course possible via highly unstable nuclear reactions, but then it would be difficult to exercise precise control over system parts.

The computational capacity estimates for carbon-based life presented here, however, do not require thermonuclear explosions. The enhancements due to weakly excited, collective quantum optical effects arise from large architectures of biological qubits (two-level systems) interacting with the electromagnetic field. These estimates for the computational capacity of superradiant life on Earth have been derived from experimental results confirming that a Lindblad-type master equation for an open quantum system in the single-photon limit effectively describes such cytoskeletal polymers. A natural question that arises is whether the quantum speed limits derived for Hermitian operators are applicable to such non-Hermitian systems. A self-consistent formulation of quantum mechanics with non-Hermitian operators and bi-orthogonal states has been developed (61), and similar bounds can be derived (1). By tracing out the electromagnetic field degrees of freedom, we arrive at an effective Hamiltonian for the quantum matter in our open system, which exhibits single-photon superradiance (1, 17).

It is important to note, however, that there is an exponentially vast discrepancy between a single-photon field and a M -photon field (62), because the scaling of their functional freedoms goes with the number of possibilities O for each field component. In a discrete space, for a field or wave function with O possibilities for each of c components at a point, we have O^c degrees of functional freedom. At two points in this space, we have $O^c \times O^c = (O^c)^2 = O^{2c}$ degrees of freedom. At all O^3 points in a three-dimensional space, we have $O^c \times O^c \times O^c \dots = (O^c)^{O^3} = O^{c \cdot O^3}$ degrees of freedom. At all O^d points in a d -dimensional space, we have $(O^c)^{O^d} = O^{c \cdot O^d}$ degrees of freedom. The functional freedom will of course be restricted by relevant constraint equations imposed by the physics. However, if, rather than in a discrete space, each of the component possibilities are $\in \mathbb{R}$, then $O \rightarrow \infty$. The granularity provided by quantum mechanics solves the problem of ultraviolet catastrophe that was tackled in the early twentieth century, by reducing the phase-space hypervolume of the field from infinite-dimensional to just a very large number. So we can see that

$$O^{a \cdot O^3} \ll O^{b \cdot O^{3M}} \quad (28)$$

where the positive values of a and b have little impact compared to the governing exponents 3 and $3M$. Thus, while the interaction of quantum matter with even a single-photon electromagnetic field produces an enormous increase in the computational capacity of life (see Eq. 14), inclusion and observation of the multiphoton field would further reduce the gap between N_E and N_Ω (see below Eq. 19).

The asymptotic scaling of the maximal superradiant decay rate for lattices of n two-level systems interacting at long range in the multiphoton excitation manifold has recently been determined in the large n limit (63), differing substantially from that expected in the Dicke limit (18). However, by operating in or near the weak-excitation limit, biological systems equipped with certain protein fibers (1, 17) may be able to isolate these fibers' collective superradiant dipole from the thermal environment, in a fashion similar to demonstrations of steady-state superradiant lasers with less than one intracavity photon. Such superradiant lasers have been shown to exhibit shielding of the nonequilibrium dipole by a factor of more than 10,000 (64).

It remains unclear, on general grounds, why a planet with carbon-based life should play a special role in the universe. First, there is the observation that the critical eukaryotic protein fibers (1, 17) discussed in this work required about 10^{10} years from the beginning for a habitable planet to form (60), and then about 10^9 years after Earth's formation for eukaryotic organisms to proliferate. Careful quantum yield measurements of these proteins, conducted in aqueous solution at thermal equilibrium (1), support the first confirmation of superradiance in a micrometer-scale biological system, whose primary function is not photosynthetic light-harvesting.

Second, on the basis of observations from the Kepler Mission (65), the number of Earth-like planets within the habitable zones of Sun-like stars could be on the order of 10^9 in the Milky Way Galaxy alone and, assuming the Milky Way is representative of all galaxies, up to about 10^{20} ($\approx m_p / m_p$) such planets could exist in the observable universe. Using the conjecture presented in Eq. 16, and assuming the scenario where all of these 10^{20} habitable planets support some form of superradiant life for a period comparable to the Earth's age, we find that the maximum computational capacity of life enlarges from t_Ω / t_p to $(t_\Omega / t_p)^{4/3} \approx 10^{80}$, about 40 orders of magnitude shy of the maximum number of elementary logical operations that can have been performed by the entire universe over its history. Such a computational enhancement for all life in the universe would increase the rate of terrestrial information processing for superradiant living systems given in Eq. 19, from about t_p^{-1} to about $(m_p / m_p) t_p^{-1} = c^3 / Gm_p \approx t_\Omega^{1/3} t_p^{-4/3}$, further underscoring the role that the quantum plays in the evolution of living matter (see the "Conjecture relating life's computational capacity to the universe's" section). If, on the other hand, we assume the more likely scenario that only a very small fraction ($10^{-20} \leq f \ll 10^0$) of such planets can support superradiant life, we find values intermediate between the conjectured Earth limit given in Eq. 14 and 10^{80} ops, scaling with $f(t_\Omega / t_p)^{4/3}$ and providing a Drake-like upper bound on the maximum number of operations that can have been performed by all Earth-like superradiant life in the universe.

Third, silicon and organosilica compounds in the interstellar medium and circumstellar clouds are common and comprise almost 10% of the molecular species in space (66), but with distinct absorption and emission features compared to aromatic quantum emitters (see the "Upper bound on the number of operations for carbon-based life on earth" section). Together with the discovery that optically

pumped SiC spin defects exhibit superradiance in their microwave photon emissions (67), these evidences lend some credence to the possibility in our universe of silicon-based superradiant life, which may exhibit alternative requirements to those we generally impose in the search for other life-supporting terrestrial planets.

There is still considerable debate about the continued applicability of Moore's law, and Neven's law is clearly a gross approximation. So too is the assumption that Earth's biomass has remained constant over multiple extinction and proliferation events. The estimates contained in this work could be altered by geothermal cycles, the age of the anthropocene, interstellar travel, discovery of other forms of life, or new energy sources, but it is unlikely that these would affect the primary conjecture and main results by more than a few orders of magnitude. Nevertheless, this work provides a starting point to understand more precisely how carbon-based life's interaction and quantum evolution with the electromagnetic field should change our estimates of eukaryotic computational capacity.

METHODS

Proof and macroscopic limit of the Margolus-Levitin theorem

Following the proof of Margolus-Levitin (2), we begin by observing that if $|\psi(0)\rangle = \sum_n c_n |E_n\rangle$, a coherent superposition of its energy eigenvectors $|E_n\rangle$, is evolved for a time t , it becomes

$$|\psi(t)\rangle = \sum_n c_n \exp(-iE_n t / \hbar) |E_n\rangle \quad (29)$$

under standard unitary evolution, and assuming a discrete spectrum. Now let

$$S(t) = \langle \psi(0) | \psi(t) \rangle = \sum_{n=0}^{\infty} |c_n|^2 \exp(-iE_n t / \hbar) \quad (30)$$

We wish to find the minimum value of t such that $S(t) = 0$. Toward this end, note that

$$\text{Re}(S) = \sum_{n=0}^{\infty} |c_n|^2 \cos(E_n t / \hbar) \quad (31)$$

Using the clever inequality $\cos x \geq 1 - (2/\pi)(x + \sin x)$, valid for all $x \geq 0$, we find that

$$\text{Re}(S) \geq \sum_{n=0}^{\infty} |c_n|^2 \left\{ 1 - \frac{2}{\pi} \left[\frac{E_n t}{\hbar} + \sin\left(\frac{E_n t}{\hbar}\right) \right] \right\} \quad (32)$$

The right-hand side of the inequality in Eq. 32, evaluated for each of the three terms in the infinite sum, is exactly equal to

$$1 - \frac{2\langle \mathcal{E} \rangle}{\pi \hbar} t + \frac{2}{\pi} \text{Im}(S) \quad (33)$$

where we have used the completeness relation $\sum_{n=0}^{\infty} |c_n|^2 = 1$, and $\langle \mathcal{E} \rangle = \sum_{n=0}^{\infty} |c_n|^2 E_n$ is the expectation value of the energy because the probability of being in an energy eigenstate $|E_n\rangle$ is $|c_n|^2$.

Clearly, for any value of t satisfying $S(t) = 0$, both $\text{Re}(S) = 0$ and $\text{Im}(S) = 0$. Substituting these after combining Eq. 32 and the expression 33, we obtain

$$1 - \frac{2\langle \mathcal{E} \rangle}{\pi \hbar} t \leq 0 \quad (34)$$

Therefore, the minimum time required for $S(t) = 0$, when the state in Eq. 29 is strictly orthogonal to the initial state $\psi(0)$, is $\tau_{\min} = \pi\hbar / 2\langle \mathcal{E} \rangle$, in agreement with Eq. 2, which completes the proof.

This bound is achievable if the spectrum includes the energy $2\langle \mathcal{E} \rangle$ and is nearly achievable if the spectrum includes an energy close to this, as would be expected for any macroscopic system, including living ones. For concreteness, let

$$|\psi(0)\rangle = \frac{1}{\sqrt{2}}(|E_0\rangle + |2\mathcal{E}\rangle) \quad (35)$$

which, assuming $E_0 = 0$ for the ground state, has average energy $\langle \mathcal{E} \rangle$. This state evolves in a time $\tau_{\min} = \pi\hbar / 2\langle \mathcal{E} \rangle$ into

$$|\psi(\tau_{\min})\rangle = \frac{1}{\sqrt{2}}(|E_0\rangle - |2\mathcal{E}\rangle) \quad (36)$$

which is, of course, orthogonal to the original state. If we evolve for the same time interval again, the state returns to $|\psi(0)\rangle$, and if evolved further will continue to oscillate between these two orthogonal states.

If we had begun with the energy-time uncertainty relation given in Eq. 1, we might have naively assumed the following (earlier) bound in terms of ΔE

$$\tau \geq \frac{\pi\hbar}{2\Delta E} \quad (37)$$

where we have made the identification $\tau = \pi\Delta t$. This earlier bound would suggest that, given a fixed average energy, one could construct a state with large enough ΔE to achieve an arbitrarily small τ . For the states in Eqs. 35 and 36, we can easily show that $\Delta E = \langle \mathcal{E} \rangle$. Using the definition $\Delta E = \sqrt{\langle H^2 \rangle - \langle H \rangle^2}$, where $H = E_0 |E_0\rangle\langle E_0| + \langle 2\mathcal{E} \rangle |2\mathcal{E}\rangle\langle 2\mathcal{E}|$ is the operator required to flip between qubit states (Eqs. 35 and 36) via the unitary evolution described in Eq. 29, we find that

$$\Delta E = \sqrt{\frac{1}{2}(E_0^2 + \langle 2\mathcal{E} \rangle^2) - \frac{1}{4}(E_0 + \langle 2\mathcal{E} \rangle)^2} = \langle \mathcal{E} \rangle - \frac{E_0}{2} \quad (38)$$

which, when the ground-state energy $E_0 = 0$, shows that $\Delta E = \langle \mathcal{E} \rangle$. Thus, in this case, both of the bounds given by Eqs. 2 and 37 are identical.

There are, of course, other cases where the Margolus-Levitin bound in Eq. 2 is much more useful than the bound given in Eq. 37. Consider the initial state

$$|\psi(0)\rangle = a[|0\rangle + |\mathcal{E}\rangle] + b[|n\mathcal{E}\rangle + |(n+1)\mathcal{E}\rangle] \quad (39)$$

where the average energy of the first pair of kets is $\langle \mathcal{E} \rangle / 2$ and the average energy of the second pair of kets is $(n + \frac{1}{2})\langle \mathcal{E} \rangle$, which will be greater than $\langle \mathcal{E} \rangle$ for all $n > 1/2$. So, we can always find coefficients a and b such that the average energy of $|\psi(0)\rangle$ is $\langle \mathcal{E} \rangle$, and respecting normalization of the state. Assuming real coefficients, $a = \sqrt{\frac{1}{2} - \frac{1}{4n}}$ and $b = \sqrt{\frac{1}{4n}}$. However, this state in Eq. 39 has a ΔE that depends on our choice of n

$$\sqrt{\left[\left(\frac{1}{2} - \frac{1}{4n}\right) + \frac{n}{4} + \frac{(n+1)^2}{4n}\right] - \left[\left(\frac{1}{2} - \frac{1}{4n}\right) + \frac{1}{4} + \frac{n+1}{4n}\right]^2} \langle \mathcal{E} \rangle = \sqrt{\frac{n}{2}} \langle \mathcal{E} \rangle \quad (40)$$

So with fixed $\langle \mathcal{E} \rangle$, $\Delta E = \mathcal{O}(\sqrt{n})\langle \mathcal{E} \rangle$ can be arbitrarily large, making the earlier lower bound in Eq. 37 contingent on the choice of n . Thus, in this case, the Margolus-Levitin bound in Eq. 2 is the more useful and universal one.

Cycles of N mutually orthogonal states and the macroscopic limit

For real systems, where arbitrarily large eigenvalues are inaccessible, we can write our initial state above Eq. 29 as a sum from $n = 0$ to $n = N - 1$. Now, we let the coefficients of that initial state $|\psi(0)\rangle$ be

$$c_n = \sqrt{\frac{E_{n+1} - E_n}{E_N}} \quad (41)$$

We will prove that for the system above an exact closed cycle of N mutually orthogonal states achieves a lower bound τ_{\min} that is only about twice the value for an oscillation between two orthogonal states.

With the definition of c_n in Eq. 41, states with degenerate energy eigenvalues are assigned a coefficient of zero and not repeated in the superposition, as the E_n values are numbered in nondecreasing order. This definition also guarantees normalized states

$$\langle \psi(0) | \psi(0) \rangle = \sum_{n=0}^{N-1} \frac{E_{n+1} - E_n}{E_N} = 1 \quad (42)$$

The average energy in the state $|\psi(0)\rangle$ is just given by

$$\langle \psi(0) | H | \psi(0) \rangle = \sum_n |c_n|^2 E_n = \sum_{n=0}^{N-1} \frac{E_{n+1} - E_n}{E_N} E_n \quad (43)$$

which in the macroscopic limit (for $N \gg 1$ and $c_n \ll 1$) can be approximated by an integral. Letting $x = n/N$ and $\epsilon(x) = E_n/E_N$, we obtain

$$\lim_{N \gg 1} \langle \psi(0) | H | \psi(0) \rangle = E_N \int_0^1 dx \epsilon \frac{d\epsilon}{dx} \frac{dn}{dx} = E_N \int_0^1 \epsilon d\epsilon = \frac{E_N}{2} \quad (44)$$

Thus, with this definition of c_n , we find an average energy for a macroscopic system that is half of its maximum energy.

Taking for simplicity the case of a one-dimensional harmonic oscillator of frequency ω and ground-state energy $E_0 = 0$, which has an exact cycle after some period $\tau = 2\pi/\omega$, all its energy eigenvalues are integer multiples of $E_1 = \hbar\omega = \hbar/\tau$, such that $E_n = nE_1$. If the system passes through its N mutually orthogonal states in one period τ , then the average time to pass between consecutive orthogonal states is $\tau_{\text{step}} = \tau/N$, noting that $E_1 \tau_{\text{step}} / \hbar = 2\pi/N$ for an exact cycle.

Substituting the harmonic oscillator spectrum $E_n = nE_1$ into Eq. 43, we find

$$\langle \mathcal{E} \rangle = \langle \psi(0) | H | \psi(0) \rangle = \frac{1}{N} \sum_{n=0}^{N-1} nE_1 = \frac{(N-1)E_1}{2} \quad (45)$$

giving the following value for the average time step between consecutive orthogonal states

$$\tau_{\text{step}} = \frac{2\pi\hbar}{NE_1} = \frac{(N-1)}{N} \frac{\pi\hbar}{\langle \mathcal{E} \rangle} \quad (46)$$

Rearranging Eq. 46 with $E_N = NE_p$, we obtain $\langle \mathcal{E} \rangle = (N-1)E_N/2N$, which in the macroscopic limit where $(N-1)/N \approx 1$ is in perfect agreement with the value derived in Eq. 44.

The state obtained from $|\psi(0)\rangle$ after m time intervals of duration τ_{step} is then

$$|\psi(m\tau_{\text{step}})\rangle = \sum_{n=0}^{N-1} \frac{1}{\sqrt{N}} \exp\left(-\frac{2\pi inm}{N}\right) |E_n\rangle \quad (47)$$

and so for two states at $M = m\tau_{\text{step}}$ and $M' = m'\tau_{\text{step}}$

$$\langle \psi(M') | \psi(M) \rangle = \sum_{n=0}^{N-1} \frac{1}{N} \exp\left[\frac{2\pi in(m'-m)}{N}\right] = \delta_{m'm} \quad (48)$$

Last, note that the inner product between the two states given in Eq. 48 can be transformed into an integral using $k = m' - m \neq 0$ and the same variable replacements as in Eq. 44

$$\lim_{N \gg 1} \langle \psi(M') | \psi(M) \rangle = \int_0^1 dx \frac{d\epsilon}{dx} \exp(2\pi i k \epsilon) = 0 \quad (49)$$

confirming that the long-cycle asymptotic computational capacity $N_{\text{max}} = (\tau_{\text{step}})^{-1} = \langle \mathcal{E} \rangle / \pi \hbar = E_{\text{max}} / h$ from Eq. 46, half the Margolus-Levitin limit in Eq. 3, is achievable in principle for any macroscopic system. For finite systems, it can be shown (2) that corrections to this limiting calculation vanish for large N , reaching the long-cycle asymptotic limit even for nearly orthogonal states. While an important result confirming the author's application of the Margolus-Levitin theorem to macroscopic systems, it is noteworthy that such factor-of-2 modifications would not affect the order-of-magnitude estimates and primary conjecture presented by the author in the main text.

REFERENCES AND NOTES

- N. S. Babcock, G. Montes-Cabrera, K. E. Oberhofer, M. Chergui, G. L. Celardo, P. Kurian, Ultraviolet superradiance from mega-networks of tryptophan in biological architectures. *J. Phys. Chem. B* **128**, 4035–4046 (2024).
- N. Margolus, L. B. Levitin, The maximum speed of dynamical evolution. *Phys. D: Nonlinear Phenom.* **120**, 188–195 (1998).
- S. Lloyd, Computational capacity of the universe. *Phys. Rev. Lett.* **88**, 237901 (2002).
- Y. Aharonov, D. Bohm, Time in the quantum theory and the uncertainty relation for time and energy. *Phys. Rev.* **122**, 1649–1658 (1961).
- Y. Aharonov, D. Bohm, Answer to fock concerning the time energy indeterminacy relation. *Phys. Rev.* **134**, B1417–B1418 (1964).
- B. Shanahan, A. Chenu, N. Margolus, A. Del Campo, Quantum speed limits across the quantum-to-classical transition. *Phys. Rev. Lett.* **120**, 070401 (2018).
- M. Okuyama, M. Ohzeki, Quantum speed limit is not quantum. *Phys. Rev. Lett.* **120**, 070402 (2018).
- S. Lloyd, Ultimate physical limits to computation. *Nature* **406**, 1047–1054 (2000).
- D. Scolnic, A. G. Riess, Y. S. Murakami, E. R. Peterson, D. Brout, M. Acevedo, B. Carreres, D. O. Jones, K. Said, C. Howlett, G. S. Anand, The Hubble tension in our own backyard: DESI and the nearness of the coma cluster. *Astrophys. J. Lett.* **979**, L9 (2025).
- A. G. Riess, W. Yuan, L. M. Macri, D. Scolnic, D. Brout, S. Casertano, D. O. Jones, Y. Murakami, G. S. Anand, L. Breuval, T. G. Brink, A. V. Filippenko, S. Hoffmann, S. W. Jha, W. D. Kenworthy, J. Mackenty, B. E. Stahl, W. Zheng, A comprehensive measurement of the local value of the Hubble constant with $1 \text{ km s}^{-1} \text{ Mpc}^{-1}$ uncertainty from the Hubble Space Telescope and the SHOES Team. *Astrophys. J. Lett.* **934**, L7 (2022).
- L. Susskind, J. Lindesay, *An Introduction to Black Holes, Information and the String Theory Revolution: The Holographic Universe* (World Scientific, 2005).
- J. D. Bekenstein, Energy cost of information transfer. *Phys. Rev. Lett.* **46**, 623–626 (1981).
- J. D. Bekenstein, Universal upper bound on the entropy-to-energy ratio for bounded systems. *Phys. Rev. D* **23**, 287–298 (1981).
- J. D. Bekenstein, Entropy content and information flow in systems with limited energy. *Phys. Rev. D* **30**, 1669–1679 (1984).
- S. Lloyd, Computational capacity of the universe. arXiv:quant-ph/0110141 (2002).
- K. Trachenko, B. Monserrat, C. J. Pickard, V. V. Brazhkin, Speed of sound from fundamental physical constants. *Sci. Adv.* **6**, eabc8662 (2020).
- H. Patwa, N. S. Babcock, P. Kurian, Quantum-enhanced photoprotection in neuroprotein architectures emerges from collective light-matter interactions. *Front. Phys.* **12**, 1387271 (2024).
- R. H. Dicke, Coherence in spontaneous radiation processes. *Phys. Rev.* **93**, 99–110 (1954).
- M. O. Scully, A. A. Svidzinsky, The super of superradiance. *Science* **325**, 1510–1511 (2009).
- Y. M. Bar-On, R. Phillips, R. Milo, The biomass distribution on Earth. *Proc. Natl. Acad. Sci. U.S.A.* **115**, 6506–6511 (2018).
- Q. Tang, W. Zheng, S. Zhang, J. Fan, L. A. Riedman, X. Hou, A. D. Muscente, N. Bykova, P. M. Sadler, X. Wang, F. Zhang, X. Yuan, C. Zhou, B. Wan, K. Pang, Q. Ouyang, N. R. McKenzie, G. Zhao, S. Shen, S. Xiao, Quantifying the global biodiversity of Proterozoic eukaryotes. *Science* **386**, eadm9137 (2024).
- A. Candalian, J. Zhen, A. G. G. M. Tielens, The aromatic universe. *Phys. Today* **71**, 38–43 (2018).
- S. Iglesias-Groth, A search for tryptophan in the gas of the IC 348 star cluster of the Perseus molecular cloud. *Mon. Not. R. Astron. Soc.* **523**, 2876–2886 (2023).
- R. L. Hudson, Interstellar tryptophan revisited. *Mon. Not. R. Astron. Soc.* **526**, 4051–4053 (2023).
- A. Dharwal, T. H. Speak, L. Zeng, A. Rashidi, B. Moore, O. Berné, A. J. Remijan, I. Schroetter, B. A. McGuire, V. M. Rivilla, A. Belloche, J. K. Jørgensen, P. Djuricin, T. Momose, I. R. Cooke, On the origin of infrared bands attributed to tryptophan in Spitzer observations of IC 348. *Astrophys. J. Lett.* **968**, L9 (2024).
- A. S. Eddington, Preliminary note on the masses of the electron, the proton, and the universe. *Math. Proc. Cambridge Philos. Soc.* **27**, 15–19 (1931).
- P. A. M. Dirac, The cosmological constants. *Nature* **139**, 323–323 (1937).
- P. A. M. Dirac, A new basis for cosmology. *Proc. R. Soc. Lond. A Math. Phys. Sci.* **165**, 199–208 (1938).
- P. A. M. Dirac, Cosmological models and the large numbers hypothesis. *Proc. R. Soc. Lond. A Math. Phys. Sci.* **338**, 439–446 (1974).
- E. P. Wigner, Relativistic Invariance And Quantum Phenomena. *Rev. Mod. Phys.* **29**, 255–268 (1957).
- P. C. W. Davies, A quantum origin of life?, in *Quantum Aspects of Life* (Imperial College Press, 2008), pp. 3–18.
- R. Landauer, Irreversibility and heat generation in the computing process. *IBM J. Res. Dev.* **5**, 183–191 (1961).
- M. Gardner, Mathematical games – The fantastic combinations of John Conway's new solitaire game "life". *Sci. Am.* **223**, 120–123 (1970).
- A. Adams, H. Zenil, P. C. W. Davies, S. I. Walker, Formal definitions of unbounded evolution and innovation reveal universal mechanisms for open-ended evolution in dynamical systems. *Sci. Rep.* **7**, 997 (2017).
- C. H. Bennett, Logical reversibility of computation. *IBM J. Res. Dev.* **17**, 525–532 (1973).
- G. Grössing, A. Zeilinger, Quantum cellular automata. *Complex Syst.* **2**, 197–208 (1988).
- W. Dür, G. Vidal, J. I. Cirac, Three qubits can be entangled in two inequivalent ways. *Phys. Rev. A* **62**, 062314 (2000).
- M. O. Scully, K. R. Chapin, K. E. Dorfman, M. B. Kim, A. Svidzinsky, Quantum heat engine power can be increased by noise-induced coherence. *Proc. Natl. Acad. Sci. U.S.A.* **108**, 15097–15100 (2011).
- M. Naruse, H. Hori, K. Kobayashi, P. Holmström, L. Thylén, M. Ohtsu, Lower bound of energy dissipation in optical excitation transfer via optical near-field interactions. *Opt. Express* **18**, A544–A553 (2010).
- J. Gao, L. Santos, G. Krishna, Z.-S. Xu, A. Iovan, S. Steinhauer, O. Gühne, P. J. Poole, D. Dalacu, V. Zwiller, A. W. Elshaari, Scalable generation and detection of on-demand W states in nanophotonic circuits. *Nano Lett.* **23**, 5350–5357 (2023).
- P. Kurian, T. Obisesan, T. Craddock, Oxidative species-induced excitonic transport in tubulin aromatic networks: Potential implications for neurodegenerative disease. *J. Photochem. Photobiol. B Biol.* **175**, 109–124 (2017).
- G. L. Celardo, M. Angeli, T. J. A. Craddock, P. Kurian, On the existence of superradiant excitonic states in microtubules. *New J. Phys.* **21**, 023005 (2019).
- L. B. Oftelie, A. De Pasquale, M. Campisi, Dynamic cooling on contemporary quantum computers. *PRX Quantum* **5**, 030309 (2024).
- P. Kurian, G. Dunston, J. Lindesay, How quantum entanglement in DNA synchronizes double-strand breakage by type II restriction endonucleases. *J. Theor. Biol.* **391**, 102–112 (2016).
- M. Gori, P. Kurian, A. Tkatchenko, Second quantization of many-body dispersion interactions for chemical and biological systems. *Nat. Commun.* **14**, 8212 (2023).
- B. Misra, E. C. G. Sudarshan, The Zeno's paradox in quantum theory. *J. Math. Phys.* **18**, 756–763 (1977).
- M. Sarkar, S. Gupta, Synchronization in the Kuramoto model in presence of stochastic resetting. *Chaos* **32**, 073109 (2022).

48. I. Nardocchia, J. Torres, M. Lechelon, V. Giliberti, M. Ortolani, P. Nouvel, M. Gori, Y. Meriguet, I. Donato, J. Preto, L. Varani, J. Sturgis, M. Pettini, Out-of-equilibrium collective oscillation as phonon condensation in a model protein. *Phys. Rev. X* **8**, 031061 (2018).

49. Z. Zhang, G. S. Agarwal, M. O. Scully, Quantum fluctuations in the Fröhlich condensate of molecular vibrations driven far from equilibrium. *Phys. Rev. Lett.* **122**, 158101 (2019).

50. K. Azizi, M. Gori, U. Morzan, A. Hassanali, P. Kurian, Examining the origins of observed terahertz modes from an optically pumped atomistic model protein in aqueous solution. *PNAS Nexus* **2**, pgad257 (2023).

51. P. W. Anderson, More is different. *Science* **177**, 393–396 (1972).

52. G. F. R. Ellis, Physics, complexity and causality. *Nature* **435**, 743–743 (2005).

53. T. Morrison *The Bluest Eye*, (New York Knopf, 1970).

54. A. W. Cross, L. S. Bishop, S. Sheldon, P. D. Nation, J. M. Gambetta, Validating quantum computers using randomized model circuits. *Phys. Rev. A* **100**, 032328 (2019).

55. Y. Zhou, E. M. Stoudenmire, X. Waintal, What limits the simulation of quantum computers? *Phys. Rev. X* **10**, 041038 (2020).

56. Google Quantum AI and Collaborators, Quantum error correction below the surface code threshold. *Nature* **638**, 920–926 (2024).

57. A. Natarajan, J. Wright, NEEXP is contained in MIP, in *2019 IEEE 60th Annual Symposium on Foundations of Computer Science (FOCS)* (IEEE, Baltimore, MD, USA, 2019), pp. 510–518.

58. F. J. Dyson, Time without end: Physics and biology in an open universe. *Rev. Mod. Phys.* **51**, 447–460 (1979).

59. P. C. W. Davies, A quantum recipe for life. *Nature* **437**, 819–819 (2005).

60. J. Barrow, F. Tipler. *The Anthropic Cosmological Principle* (Oxford Univ. Press, 1988).

61. Moiseyev, N. *Non-Hermitian Quantum Mechanics* (Cambridge Univ. Press, 2011).

62. Penrose, R. *Fashion, Faith, and Fantasy in the New Physics of the Universe* (Princeton Univ. Press, 2016).

63. W.-K. Mok, A. Poddar, E. Sierra, C. C. Rusconi, J. Preskill, A. Asenjo-Garcia, Universal scaling laws for correlated decay of many-body quantum systems. arXiv:2406.00722 (2024).

64. J. G. Bohnet, Z. Chen, J. M. Weiner, D. Meiser, M. J. Holland, J. K. Thompson, A steady-state superradiant laser with less than one intracavity photon. *Nature* **484**, 78–81 (2012).

65. S. Bryson, M. Kunimoto, R. K. Kopparapu, J. L. Coughlin, W. J. Borucki, D. Koch, V. S. Aguirre, C. Allen, G. Barentsen, N. M. Batalha, T. Berger, A. Boss, L. A. Buchhave, C. J. Burke, D. A. Caldwell, J. R. Campbell, J. Catanzarite, H. Chandrasekaran, W. J. Chaplin, J. L. Christiansen, J. Christensen-Dalsgaard, D. R. Ciardi, B. D. Clarke, W. D. Cochran, J. L. Dotson, L. R. Doyle, E. S. Duarte, E. W. Dunham, A. K. Dupree, M. Endl, J. L. Fanson, E. B. Ford, M. Fujieh, T. N. Gautier III, J. C. Garry, R. L. Gilliland, F. R. Girouard, A. Gould, M. R. Haas, C. E. Henze, M. J. Holman, A. W. Howard, S. B. Howell, D. Huber, R. C. Hunter, J. M. Jenkins, H. Kjeldsen, J. Kolodziejczak, K. Larson, D. W. Latham, J. Li, S. Mathur, S. Meibom, C. Middour, R. L. Morris, T. D. Morton, F. Mullally, S. E. Mullally, D. Fletcher, A. Prsa, S. N. Quinn, E. V. Quintana, D. Ragozzine, S. V. Ramirez, D. T. Sanderfer, D. Sasselov, S. E. Seader, M. Shabram, A. Shporer, J. C. Smith, J. H. Steffen, M. Still, G. Torres, J. Troeltzsch, J. D. Twicken, A. K. Uddin, J. E. Van Cleve, J. Voss, L. M. Weiss, W. F. Welsh, B. Wohler, K. A. Zamudio, The occurrence of rocky habitable-zone planets around solar-like stars from Kepler data. *Astron. J.* **161**, 36 (2021).

66. N. Job, K. Thirumooorthy, Silicon chemistry in the interstellar medium and circumstellar envelopes. *ACS Earth Space Chem.* **8**, 467–482 (2024).

67. A. Gottscholl, M. Wagenhöfer, M. Klimmer, S. Scherbel, C. Kasper, V. Baianov, G. V. Astakhov, V. Dyakonov, A. Sperlich, Superradiance of spin defects in silicon carbide for maser applications. *Front. Photon.* **3**, 886354 (2022).

Acknowledgments: Portions of this manuscript were presented and discussed at the Quantum Biology Gordon Research Conference 2025 in Italy, at the Quantum Thermodynamics 2024 Conference in Maryland, at the Molecular Biophysics Workshop 2024 in France, at the Princeton-Texas A&M Quantum Summer School 2023 in Wyoming, at the Quantum Biology Gordon Research Conference 2023 in Texas, and during the author's residencies as a Fellow of the UCSB Kavli Institute for Theoretical Physics in 2023–2024 and as a Simons Scholar at the UCLA Institute for Pure and Applied Mathematics in 2022. High-performance computing resources from the Oak Ridge and Argonne Leadership Computing Facilities made the prior numerical simulations of superradiance in large protein systems (1, 17) possible. Last, the author wishes to thank the anonymous reviewers for their helpful questions and comments. **Funding:** The author wishes to acknowledge the partial financial supports of the Howard University Graduate School, the Alfred P. Sloan Foundation, the Guy Foundation, the Chaikin-Wile Foundation, and the National Science Foundation. High-performance computing resources were provided by the Leadership Computing Facilities at Argonne National Laboratory and Oak Ridge National Laboratory. The Kavli Institute for Theoretical Physics (KITP) and the Institute for Pure and Applied Mathematics (IPAM) are supported by grants from the National Science Foundation. **Author contributions:** P.K. conceptualized the arguments and wrote the paper. **Data and materials availability:** All data needed to evaluate the conclusions in the paper are present in the paper. **Competing interests:** The author declares that they have no competing interests.

Submitted 30 October 2024

Accepted 24 February 2025

Published 28 March 2025

10.1126/sciadv.adt4623